CHAPTER 1

General Introduction

In vivo visualization and quantification of biochemical processes and structures of the human body is important for understanding mechanisms underlying disease and normal body processes. While x-ray, computed tomography (CT), and magnetic resonance imaging (MRI) are valuable approaches to image anatomical structures, for the underlying physiological time-varying mechanisms, molecular imaging techniques are needed.

Amongst all available molecular imaging techniques, positron emission tomography (PET) is the most specific and sensitive method.[1] This technique requires the injection of a tracer amount of a compound labelled with a positron emitting radionuclide. After injection, this radiotracer is distributed throughout the body according to the characteristics of the (labelled) compound. The radionuclide decays to a stable state by emitting a positron, which travels only a very short distance before colliding with a free electron. The combination of positron and electron is unstable, resulting in the annihilation of both particles, and the simultaneous emission of two high-energy photons. These photons travel in essentially opposite directions and can be simultaneously detected (coincidence detection) outside the body by the ring of detectors of the PET scanner. The detection of these photons can then be translated into 3D images, showing the distribution of the radiotracer within the body, reflecting the biochemical process under study.[2]

There are many different processes within the body that can be visualised using different radiotracers. For example, tissue metabolism can be measured using the glucose analogue [^{18}F]-2-fluoro-2-deoxy-D-glucose (FDG). Images provided by this radiotracer may show metabolic abnormalities, which might be the consequence of a disease.[3] Furthermore, cancerous cells are also known to consume more glucose than normal tissue and, therefore, FDG can also be used for the visualisation of tumours throughout the body.[4] Moreover, metastatic prostate cancer can be imaged using the prostate-specific membrane antigen using [^{68}Ga]PSMA.[5] In the brain sero-

tonin transporter and neuroinflammation may, for example, be assessed by other radiotracers such as [^{11}C]DASB,[6] and (*R*)-[^{11}C]PK11195 or [^{11}C]PBR28,[7] respectively, which are relevant targets in depression, brain injury, and neurodegeneration studies. With these many applications, PET can be an important tool not only for clinical diagnosis and disease staging, but also for monitoring disease progression, response during therapy, and drug development.[8]

Neurodegeneration

PET imaging with different radiotracers may be used for diagnostic purposes in dementia and for studying the pathophysiological processes in neuronal decay. Neurodegeneration is characterized by a progressive loss of neuronal function up to, and including, neuronal death. Although neurodegeneration is a common feature of several diseases, the exact reason for such an elevated neuronal loss is not completely clear. A consequence of this process, when it goes beyond normal ageing, is the gradual loss of cognitive abilities, resulting in dementia.[9] Dementia is a symptom that can be associated with several diseases, although it may present itself differently.[3]

Studies have already shown that neurodegeneration is correlated with a reduction in cerebral glucose consumption.[3;10] Therefore, glucose imaging is a suitable tool for the visualization of hypometabolism caused by a disease, and it may aid clinicians with identifying different diseases earlier and more accurately, since each one presents itself in a different form. As an example, while patients with Parkinson's disease show decreased metabolic brain activity (hypometabolism) contralateral to the affected body side in the prefrontal cortex, anterior cingulate, gyrus and a few parietal and occipital regions, patients diagnosed with dementia with Lewy Bodies showed hypometabolic activity in the occipital lobe, parietotemporal, and frontal re-

gions.[3]

Alzheimer's Disease

The most common form of dementia is Alzheimer's Disease (AD), which accounts for 60-70% of all cases.[9] In the clinic, AD typically presents itself with a decline in memory, but it can also show decay in other cognitive domains, such as executive functioning, orientation in time and space, and language.[11] This disease usually starts by showing symptoms in elderly people above 60 years of age, but it can also have an early onset, where people between 30 and 60 years present symptoms. In clinical practice, often a Mini-Mental State Examination (MMSE) is used to measure cognitive impairment. This is a 30-point questionnaire where patients with a score below 24 are considered cognitively impaired.[12] Furthermore, AD patients usually show a reduction in hippocampal volume,[13] reduced brain metabolism,[14] and abnormal deposition of amyloid-β (Aβ) plaques and neurofibrillary tau tangles in the brain.[15] These deposits can be verified in a post-mortem examination using immunohistochemical staining of Aβ and tau tangles.[15] Studies have shown that Aβ deposition is the first abnormality in the brain of cognitively normal people who eventually may develop AD, followed by tau aggregations and, then, changes in brain structure.[15] It takes many years between the first appearance of Aβ deposits and the first symptoms. Furthermore, some cognitively normal elderly people might also present some amyloid load.[16]

In research settings, a framework was established for a clear definition of AD, considering Aβ plaques and tau tangles as the main biomarkers for differentiating AD from other neurodegenerative diseases.[17] The same framework also introduced the term 'Alzheimer's continuum spectrum' to define all subjects who present with abnormal Aβ deposits, whilst the term 'Alzheimer's Disease' was used only for patients who present with both Aβ plaques and tau

neurofibrillary tangles.[17]

As PET enables *in vivo* imaging of a broad range of functional processes, it is an important tool not only to aid clinicians in the diagnosis of AD, but also to assist in the correct identification of cohorts of patients in research and drug development studies. The importance of accurately selecting AD patients and subjects that are in an early stage of the disease is critical for drug intervention early during the disease process when cognition is not yet too much affected.[10;17]

All previously described changes in the brain of AD patients can be visualised *in vivo* using either PET (for functional changes) or MRI (for anatomical changes) imaging techniques. As previously mentioned, AD is a neurodegenerative disease that results in a reduction in cerebral glucose consumption. FDG PET is a useful tool for the identification of hypometabolic brain, and it has previously been reported that these reductions start happening years before clinical symptoms.[18] When compared with age-matched healthy volunteers, the main regions that show metabolic reductions are the parietotemporal, frontal, and posterior cingulate cortices. Furthermore, these reductions become more pronounced with disease progression and they are associated with a decrease in cognitive test scores.[14] Figure 1.1 shows typical FDG scans for an AD patient and a healthy volunteer.

[^{11}C]labelled Pittsburgh Compound B (PIB) was one of the first radiotracers developed for in vivo imaging of Aβ plaques in the brain.[19] More recently, other radiotracers such as [^{18}F]florbetapir, [^{18}F]florbetaben, and [^{18}F]flutemetamol, have been developed for Aβ imaging,[20] but PIB remains the gold standard. PET scans of AD patients have shown generally increased cortical and subcortical uptake when compared with healthy controls, who show a higher binding of PIB in white matter regions when compared to grey matter (Figure 1.1). Aβ-deposition has been shown to happen in phases, affecting

different parts of the brain following a distinct sequence: starting at the neocortex; moving to allocortical regions, then the diencephalic nuclei, the striatum, and the cholinergic nuclei of the basal forebrain, with the brainstem becoming involved in the next stage, and, finally, the cerebellum.[21]

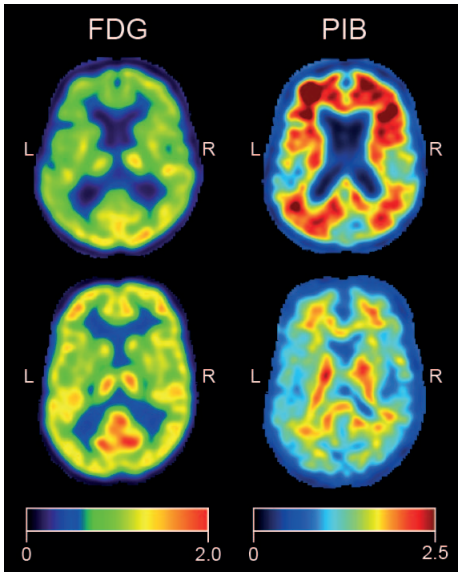

Figure 1.1: Typical FDG (left column) and PIB (right column) patterns of an AD patient (top row) and an age-matched healthy control (bottom row). Colour scales were adjusted to the same range.

Mild Cognitive Impairment

Mild cognitive impairment (MCI) is an intermediate stage between healthy individuals and demented patients. In this stage, patients start having cognitive complaints, but these do not (yet) affect the performance of daily activities.[22] Some MCI patients may present elevated Aβ deposits when compared with healthy controls, while others show close to no deposition. According to the new framework for classification, these first patients are part of the Alzheimer

spectrum, but are not yet considered to be AD patients. Longitudinal studies suggest that most of these patients with Aβ deposits ultimately convert to AD.[23] Moreover, it has been estimated that 30% of MCI patients eventually convert, at an annual rate of 10 to 15%.[24]

Both FDG and PIB PET scans are also useful for distinguishing MCI patients from healthy controls. However, changes in amyloid retention, and thus in PIB signal, are more pronounced than changes in glucose consumption,[25] making it easier to distinguish between both diagnoses on the basis of PIB scans rather than FDG scans.

PET Quantification and Data Analysis

Visual Assessment

For clinical diagnostic purposes, visual assessment of PET scans suffices in most cases. In this scenario, a PET scan is acquired over a brief period of time (e.g. 20 to 30 minutes acquisition), usually around 30 to 60 minutes after tracer injection. The high-quality static (i.e. single) image shows cerebral tracer uptake. With this, clinicians can assess the presence of disease by the decreased or increased uptake of the radiotracer also considering total brain uptake pattern, for example. However, visual assessment of images relies on the expertise of the clinician and it is subject to observer variability.[26;27] This assessment can also be performed using semi-quantitative approaches.

Semi-Quantitative Approaches

The most commonly used approach to standardize the uptake in static PET images is by using the Standardized Uptake Values (SUV). This parameter is calculated by dividing the measured activity concentration in tissue by the

ratio of injected activity and body weight of the subject (either total or lean body mass). When a reference region is available (i.e. a region where no specific binding of the tracer occurs), a ratio with the average value of this region (SUVR) can be used. This normalization process allows for the comparison of tracer uptake between subjects and studies.

However, SUV and SUVR are standardized measures of total radiotracer uptake at the time of the scan. This means that although the concentration of radioactivity measured by the PET scanner is normalized, it does not discriminate between the possible sources of the signal, such as specific uptake and uptake in blood (Figure 1.2). Hence, these measures are only semi-quantitative. Sometimes semi-quantitative scans are also acquired at the same time of tracer injection. In this case, the PET acquisition is started at the same time and the scan may last from 10 to 20 minutes. These images are often considered as measurements of blood flow. Moreover, tracers that target P-glycoprotein, an efflux transporter of the blood-brain barrier, such as [^{11}C]Verapamil and [^{18}F]MC225, are recommended to be scanned with shorter acquisition times, for example.[28;29]

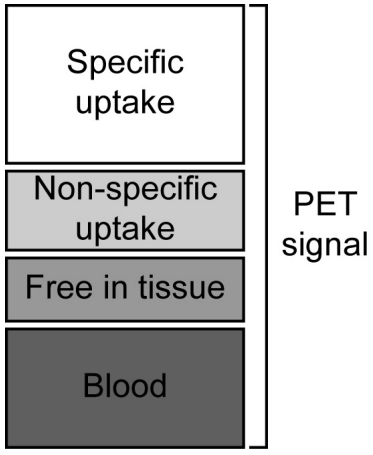

Figure 1.2: Possible partition of the PET signal in tissue.

Quantitative Approaches

An example to illustrate the importance of accurate parameter quantification is the neurokinin-1 receptor status study by Wolfensberger and colleagues.[30] In this study, PET scans were performed in a group of healthy volunteers before and after the oral administration of an antagonist of this receptor. Figure 1.3 shows SUV images (first row) and quantitative (specific) binding potential (BP_{ND}) images (bottom row) before (first column) and after (right column) administration of the antagonist aprepitant. In this example, the quantitative images show almost complete blocking of the receptor in the striatum, while SUV images still show considerable uptake (which, in fact, represents non-specific binding). Therefore, in this case, SUV images, in this case, are misleading, resulting in incorrect estimation of tracer binding.

To quantitatively measure a (patho)physiological process, a dynamic PET scan is required. Instead of a short static acquisition, a series of 3D scans is acquired and reconstructed at different intervals of the total duration of the scan. This 4D (3D in space plus 1D of time) set of images reflects the dynamic uptake of the tracer by the tissue under study, starting at the time of injection. This allows for the generation of time-activity curves (TACs) that describe radiotracer accumulation over time for a specific voxel or group of voxels. These curves display the dynamic behaviour (pharmacokinetics) of the injected compound, from the initial influx in tissue to retention and/or washout at the end of the scan. A mathematical model can be fitted to these data, thereby translating these radioactivity measurements into parameters that best describe the underlying biological processes, such as perfusion and receptor density.[2]

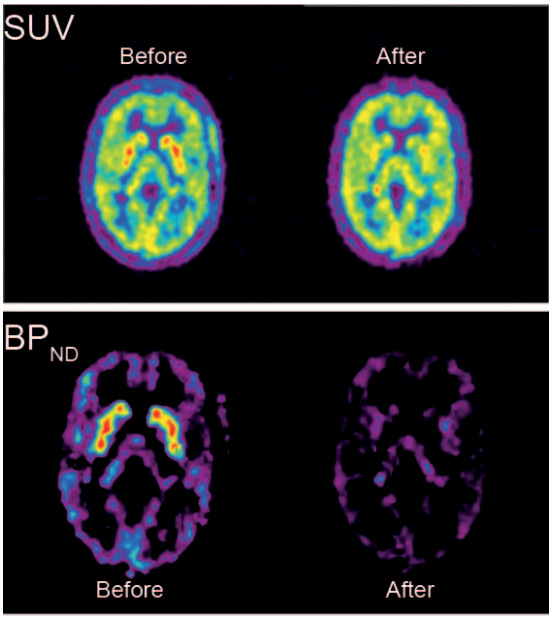

Figure 1.3: Two sets of images from the same 90 minutes [^{11}C]R116301 scans of a healthy subject before (left column) and after (right column) a 125 mg oral dose of aprepitant. SUV images (top row), based on a static portion (60 – 90 minutes after tracer injection) of the 90 minutes scan, show a significant contribution from nonspecific binding. Parametric binding potential (BP_{ND}) images (bottom row) based on kinetic analysis of the entire dynamic 90 minutes scan show nearly complete blocking (97%) by aprepitant. (adapted from Lammertsma et al. Forward to the Past: The Case for Quantitative PET Imaging, J Nucl Med. 2017; 58:1019-1024 © SNMMI[31])

However, depending on kinetics, most dynamic scans last longer and might be too burdensome for some subjects, such as Parkinson's disease and ataxia patients, who suffer from tremors, or dementia patients, who might get confused in the middle of the scan. In addition, dynamic scans are more expensive (considering time, resources, and money) than static scans.[31] Nevertheless, the advantages of a dynamic scan surpass its drawbacks. While a static scan will produce an image of net radiotracer uptake, it cannot fully

identify specific from non-specific uptake. Recent studies have already shown substantial differences between full quantification and standardized measures of radiotracer uptake, demonstrating that the latter might be misleading.[30–32] Moreover, the advantages of performing visual assessment using quantitative images instead of semi-quantitative ones have also been shown.[27] This is due to the fact that net uptake is a complex exchange of influx, retention, and clearance of the radiotracer between plasma and tissue. Importantly, adequate analysis of a dynamic scan provides extra and more accurate information than a single static scan,[33] reducing the number of subjects that need to be included in a study or the number of scans that a patient may need to undergo for a correct diagnosis. Thus, there is a reduction in exposure of subjects to radiation.[31] In addition, a time-weighted average of specific time frames from dynamic PET scans can be made so that static SUV and SUVR images can also be generated when needed.

Pharmacokinetic Analysis

The goal of pharmacokinetic modelling of dynamic PET data is to obtain quantitative values that characterize the biological process under study. This approach will convert radioactivity measurements into quantitative values of the model's parameters. However, these models require an arterial blood or plasma input function, which is the time-activity curve of plasma. Usually, this function is measured through blood sampling. Each subject has its own input function taken into consideration and, therefore, pharmacokinetic modelling can correctly account for between-subject variations.[34] However, blood sampling may be uncomfortable for subjects, and it is mainly used in research studies and not in a clinical setting.

For PET studies, the most commonly used models to describe the behaviour of a radiotracer are compartment models.[35] Each compartment does not necessarily describe a tissue where the tracer is located, but rather a

kinetic 'state'. In other words, it describes how the tracer uptake changes over time, but not in space.[34] PET measurements reflect the total uptake in tissue, but this measure can be split in different 'state' concentrations (Figures 1.2 and 1.4), such as in a compartment that expresses the amount of specifically bound tracer, and a compartment for free tracer in tissue. The number of compartments to be used in the model does not only depend on the radiotracer, but also on both statistical noise and the underlying physiological process.[35] There is no universal model that may fit all radiotracers, thus requiring a full study of pharmacokinetics for every newly developed radiotracer.

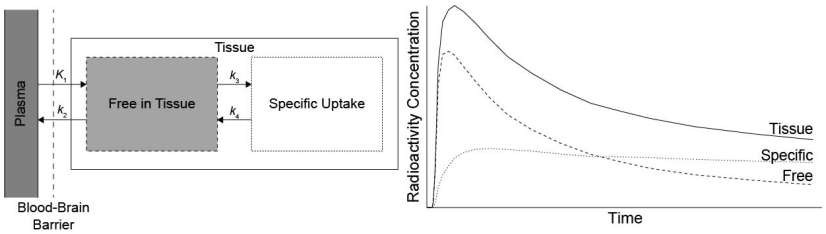

Figure 1.4: Schematic representation of a model with two compartments (left) in brain tissue (one for free radiotracer in tissue and another for specific uptake), and the rate constants describing exchange between plasma and tissue (K_1 and k_2) and between tissue compartments (k_3 and k_4). TAC measured (right) for the tissue (solid line), and its decomposition into TACs for each compartment of the model.

Reference Tissue Models

To overcome the disadvantages of measuring the arterial input function, reference tissue models have been developed. These models are based on the assumption that there is a region, with similar characteristics as the tissue of interest, but devoid of the specific target for the injected radiotracer. Measurements of these regions can then be used as an indirect input function to estimate model parameters. Although there are clear advantages of reference

tissue models, it should be emphasized that these models are simplifications of blood-input models and can, therefore, only be used after validation against the gold-standard blood-input model.

The most common of these models is the Simplified Reference Tissue Model (SRTM).[36] It assumes that there is rapid exchange of the radiotracer between free and non-specific compartments. Therefore, the TAC of the target tissue can be sufficiently fitted by a single compartment model with arterial input. SRTM is also based on the assumption that the ratio between influx and clearance in the reference region is the same as in the region under study, i.e. the volume of distribution of the non-specific bound tracer in the reference tissue is the same as in the target. This model results in three parameters: relative tracer influx (R_1), BP_{ND}, and rate constant for transfer from tissue to plasma compartment (k_2).[36] These parameters are measures related to relative regional cerebral blood flow of target tissues, specific binding of the radiotracer to its target (e.g. receptor), and washout rate of the radiotracer from tissue to plasma, respectively.

The Simplified Reference Tissue Model 2 (SRTM2)[37] was developed to further reduce noise in the estimation of SRTM parameters. This model is based on the fact that the clearance constant of the reference region ($k_2^{'}$) is the same independently of the target region being modelled. The fitting of this model happens in two stages: firstly, SRTM is fitted to all regions, and then the resulting parameters from the first fit are used as input for a second fit, taking the median $k_2^{'}$ parameter value for all regions of the study.[37] With this parameter fixed, the total number of parameters that need to be assessed by the model is reduced. With this approach, a better accuracy and precision can be achieved in most cases.[38]

It is worth mentioning that these models, while originally developed to be applied at a regional level, can also be used for each voxel. Then,

a parametric image will be generated for each parameter estimated by the model.[39] These quantitative parametric images allow for the assessment of a parameter with the spatial resolution of the scanner.

Image and Data Analysis

After obtaining (semi-)quantitative images, interpretation of these images is performed for e.g. diagnosis and assessment of disease progression or treatment efficacy. As previously mentioned, visual inspection of images heavily relies on the reader's expertise and is susceptible to inter- and intra-reader variability, especially when there are subtle changes.[26] Therefore, quantitative analyses approaches are essential. Apart from being a sensitive technique to monitor disease progression and response to therapy, PET data can also be used to correlate changes in image data with clinical evaluation.

Regional Analysis

The simplest approach to retrieve data from (semi-)quantitative PET images is through the use of Volumes of Interest (VOIs). These VOIs can be drawn manually, through automated procedures, or based on pre-defined anatomical structures. Usually, the average uptake value of all the voxels within a VOI is taken. This is the most common method used in brain studies, since it allows for the researcher to focus on regions that are mostly affected by a disease, comparing uptake between groups of patients and controls. However, the spatial resolution of PET cameras can be a limiting factor, when the focus of the study is on small regions, which may be affected by spill-in from nearby tissues (partial volume effect) thus 'contaminating' the average value of that VOI.[40] Another approach for small VOIs is to retrieve the maximum value inside a VOI, an approach most frequently used in oncology studies.

Voxel-Based Analysis

Instead of dividing an image into VOIs, (semi-)quantitative PET images can be analysed by visual assessment or by statistical models at a voxel level. The latter results in image maps that show which cluster of voxels present a statistically significant difference between groups. Unfortunately, in this univariate type of analysis, voxels are tested independently, largely ignoring possible connections within the brain. Furthermore, this is an approach used mainly for the comparison of groups of subjects. Yet, a single subject analysis can be done by comparing the subject's image to a database of healthy controls, as it was done to predict conversion to dementia[41] or to identify probable patients.[42]

Scaled Subprofile Model

Regions of the brain are known to be connected with each other and, therefore, the brain can be viewed as a network. The Scale Subprofile Model (SSM) using Principal Component Analysis (PCA) is an approach that identifies abnormal patterns in images.[43] By using a multivariate approach, this technique may identify subtler changes that univariate techniques, such as SPM, may not. SSM/PCA is based on a series of steps that starts with the intensity normalization of voxel values. Next, the average value within and between subjects is subtracted, so that only the residuals remain. Then PCA is applied and the principal components are combined to create a final disease pattern (DP). This DP contains voxels that show the main differences between a group of patients and healthy controls: regions of the brain where there is an increase or a decrease of the measured input. In addition to better understanding the pathophysiology, the DP can also be used for single subject assessment, providing individual assessment of subjects that were not used to generate the DP. The image of a new subject is compared to the DP, resulting in a score

that reflects the similarity between them which may aid with subject diagnosis: the higher the score, the more comparable they are. SSM/PCA can be applied to different types of neuroimaging techniques and can be used to obtain characteristic DP for a diverse range of diseases.[44] While this approach has already been used to generate DPs for Alzheimer's[45] and Parkinson's[43] diseases, its use has been restricted mainly to FDG PET scans. Therefore, it is of great interest to see its performance with different radiotracers or in combination with fully quantitative images.

Thesis Aim

The aim of this thesis is to further explore the possibilities of using quantitative images in neuroimaging PET studies of Alzheimer's disease patients. To this end, three goals were set:

1. to improve parameter estimations for studies involving PIB PET dynamic scans,
2. to use resulting parametric maps also as a surrogate for FDG PET scans,
3. to explore the use of parametric images as input data in SSM/PCA analyses.

Thesis Outline

Chapter 2 aims to improve parameter estimation of the efflux rate in pharmacokinetic studies using a reference tissue model, including an assessment of the consequences of wrong estimates of the parameter in $BP_{ND}$and R_1.

Chapter 3 explores the similarities between metabolic uptake values measured through semi-quantitative FDG images (SUVR) and quantita-

tive images of regional cerebral blood flow estimated though dynamic PIB PET scans. Furthermore, in **Chapter 4**, the performance of these two types of images is tested in an automated diagnostic software package, developed for diagnosing of Alzheimer's disease.

Chapter 5 presents the use of SSM/PCA in combination with parametric images derived from pharmacokinetic modelling. Finally, **Chapter 6** explores differences and similarities between DPs generated by semi-quantitative images (FDG SUVR) and quantitative images of regional cerebral blood flow.

Chapter 7 provides a summary of the results of this thesis (**Chapter 8** provides the same summary in Dutch), and **Chapter 9** presents an overall discussion and potential future research directions.

Bibliography

[1] Terry Jones and David Townsend. History and future technical innovation in positron emission tomography. *Journal of Medical Imaging*, 4(1):011013, mar 2017.

[2] Juan José Vaquero and Paul Kinahan. Positron Emission Tomography: Current Challenges and Opportunities for Technological Advances in Clinical and Preclinical Imaging Systems. *Annual Review of Biomedical Engineering*, 17(1):385–414, dec 2015.

[3] Laura K. Teune, Anna L. Bartels, Bauke M. De Jong, Antoon T.M. Willemsen, Silvia A. Eshuis, Jeroen J. De Vries, Joost C.H. Van Oostrom, and Klaus L. Leenders. Typical cerebral metabolic patterns in neurodegenerative brain diseases. *Movement Disorders*, 25(14):2395–2404, 2010.

[4] Eric M. Rohren, Timothy G. Turkington, and R. Edward Coleman. Clinical Applications of PET in Oncology. *Radiology*, 231(2):305–332, may 2004.

[5] Tobias Maurer, Matthias Eiber, Markus Schwaiger, and Jürgen E. Gschwend. Current use of PSMA–PET in prostate cancer management. *Nature Reviews Urology*, 13(4):226–235, apr 2016.

[6] Peter A. Shapiro, Richard P. Sloan, Chetram Deochand, Ana M. Franceschi, Christine Delorenzo, J. John Mann, and Ramin V. Parsey. Quantifying serotonin transporters by PET with [^{11}C]-DASB before and after interferon-α treatment. *Synapse*, 68(11):548–555, nov 2014.

[7] Federico E. Turkheimer, Gaia Rizzo, Peter S. Bloomfield, Oliver Howes, Paolo Zanotti-Fregonara, Alessandra Bertoldo, and Mattia Veronese. The methodology of TSPO imaging with positron emission tomography. *Biochemical Society Transactions*, 43(4):586–592, aug 2015.

[8] C. J. Bench, A. A. Lammertsma, R. J. Dolan, P. M. Grasby, S. J. Warrington, K. Gunn, M. Cuddigan, D. J. Turton, S. Osman, and R. S. J. Frackowiak. Dose dependent occupancy of central dopamine D2 receptors by the novel neuroleptic CP-88,059-01: a study using positron emission tomography and ^{11}C-raclopride. *Psychopharmacology*, 112(2-3):308–314, sep 1993.

[9] A. Burns and S. Iliffe. Alzheimer's disease. *BMJ*, 338(feb05 1):b158–b158, feb 2009.

[10] Agneta Nordberg, Juha O Rinne, Ahmadul Kadir, and Bengt Långström. The use of PET in Alzheimer disease. *Nature reviews. Neurology*, 6(2):78–87, 2010.

[11] G. McKhann, D. Drachman, M. Folstein, R. Katzman, D. Price, and E. M. Stadlan. Clinical diagnosis of Alzheimer's disease: Report of the NINCDS-ADRDA Work Group* under the auspices of Department of Health and Human Services Task Force on Alzheimer's Disease. *Neurology*, 34(7):939–939, jul 1984.

[12] Verna C. Pangman, Jeff Sloan, and Lorna Guse. An examination of psychometric properties of the Mini-Mental State Examination and the Standardized Mini-Mental State Examination: Implications for clinical practice. *Applied Nursing Research*, 13(4):209–213, nov 2000.

[13] M. Bobinski, M.J. de Leon, J. Wegiel, S. DeSanti, A. Convit, L.A. Saint Louis, H. Rusinek, and H.M. Wisniewski. The histological validation of post mortem magnetic resonance imaging-determined hippocampal volume in Alzheimer's disease. *Neuroscience*, 95(3):721–725, dec 1999.

[14] Aoife Hunt, Peter Schönknecht, Marcus Henze, Ulrich Seidl, Uwe Haberkorn, and Johannes Schröder. Reduced cerebral glucose metabolism in patients at risk for Alzheimer's disease. *Psychiatry Research: Neuroimaging*, 155(2):147–154, jul 2007.

[15] H. Braak and E. Braak. Neuropathological stageing of Alzheimer-related changes. *Acta Neuropathologica*, 82(4):239–259, sep 1991.

[16] Geert De Meyer, Fred Shapiro, Hugo Vanderstichele, Eugeen Vanmechelen, Sebastiaan Engelborghs, Peter P. De Deyn, Els Coart, Oskar Hansson, Lennart Minthon, Henrik Zetterberg, Kaj Blennow, Leslie Shaw, John Q. Trojanowski, and Alzheimer's Disease Neuroimaging Initiative. Diagnosis-Independent Alzheimer Disease Biomarker Signature in Cognitively Normal Elderly People. *Archives of Neurology*, 67(8):949, aug 2010.

[17] Clifford R. Jack, David A. Bennett, Kaj Blennow, Maria C. Carrillo, Billy Dunn, Samantha Budd Haeberlein, David M. Holtzman, William Jagust, Frank Jessen, Jason Karlawish, Enchi Liu, Jose Luis Molinuevo, Thomas Montine, Creighton Phelps, Katherine P. Rankin, Christopher C. Rowe, Philip Scheltens, Eric Siemers, Heather M. Snyder, Reisa Sperling, Cerise Elliott, Eliezer Masliah, Laurie Ryan, and Nina Silverberg. NIA-AA Research Framework: Toward a biological definition of Alzheimer's disease. *Alzheimer's & Dementia*, 14(4):535–562, apr 2018.

[18] Lisa Mosconi, Rachel Mistur, Remigiusz Switalski, Wai Hon Tsui, Lidia Glodzik, Yi Li, Elizabeth Pirraglia, Susan De Santi, Barry Reisberg, Thomas Wisniewski, and Mony J. de Leon. FDG-PET changes in brain glucose metabolism from normal cognition to pathologically verified Alzheimer's disease. *European Journal of Nuclear Medicine and Molecular Imaging*, 36(5):811–822, may 2009.

[19] William E Klunk, Henry Engler, Agneta Nordberg, Yanming Wang, Gunnar Blomqvist, Daniel P Holt, Mats Bergström, Irina Savitcheva, Guo-feng Huang, Sergio Estrada, Birgitta Ausén, Manik L Debnath, Julien Barletta, Julie C Price, Johan Sandell, Brian J Lopresti, Anders Wall, Pernilla Koivisto, Gunnar Antoni, Chester A Mathis, and Bengt Långström. Imaging brain amyloid in Alzheimer's disease with Pittsburgh Compound-B. *Annals of neurology*, 55(3):306–19, mar 2004.

[20] Elizabeth Morris, Anastasia Chalkidou, Alexander Hammers, Janet Peacock, Jennifer Summers, and Stephen Keevil. Diagnostic accuracy of ^{18}F amyloid PET tracers for the diagnosis of Alzheimer's disease: a systematic review and meta-analysis. *European Journal of Nuclear Medicine and Molecular Imaging*, 43(2):374–385, 2016.

[21] Dietmar R. Thal, Udo Rüb, Mario Orantes, and Heiko Braak. Phases of Aβ-deposition in the human brain and its relevance for the development of AD. *Neurology*, 58(12):1791–1800, jun 2002.

[22] Ronald C. Petersen, Rachelle Doody, Alexander Kurz, Richard C. Mohs, John C. Morris, Peter V. Rabins, Karen Ritchie, Martin Rossor, Leon Thal, and Bengt Winblad. Current Concepts in Mild Cognitive Impairment. *Archives of Neurology*, 58(12):1985, dec 2001.

[23] A. Okello, J. Koivunen, P. Edison, H. A. Archer, F. E. Turkheimer, K. Nagren, R. Bullock, Z. Walker, A. Kennedy, N. C. Fox, M. N. Rossor, J. O. Rinne, and D. J. Brooks. Conversion of amyloid positive and negative MCI to AD over 3 years: An ^{11}C-PIB PET study. *Neurology*, 73(10):754–760, sep 2009.

[24] Charles DeCarli. Mild cognitive impairment: prevalence, prognosis, aetiology, and treatment. *The Lancet Neurology*, 2(1):15–21, jan 2003.

[25] Anton Forsberg, Henry Engler, Ove Almkvist, Gunnar Blomquist, Göran Hagman, Anders Wall, Anna Ringheim, Bengt Långström, and Agneta Nordberg. PET imaging of amyloid deposition in patients with mild cognitive impairment. *Neurobiology of Aging*, 29(10):1456–1465, oct 2008.

[26] Silvia Morbelli, Andrea Brugnolo, Irene Bossert, Ambra Buschiazzo, Giovanni B. Frisoni, Samantha Galluzzi, Bart N.M. Van Berckel, Rik Ossenkoppele, Robert Perneczky, Alexander Drzezga, Mira Didic, Eric Guedj, Gianmario Sambuceti, Gianluca Bottoni, Dario Arnaldi, Agnese Picco, Fabrizio De Carli, Marco Pagani, and Flavio Nobili. Visual Versus semi-quantitative analysis of ^{18}F-FDG-PET in Amnestic MCI: An European Alzheimer's Disease Consortium (EADC) project. *Journal of Alzheimer's Disease*, 44(3):815–826, 2015.

[27] Lyduine E. Collij, Elles Konijnenberg, Juhan Reimand, Mara ten Kate, Anouk den Braber, Isadora Lopes Alves, Marissa Zwan, Maqsood Yaqub, Daniëlle M.E. van Assema, Alle Meije Wink, Adriaan A. Lammertsma, Philip Scheltens, Pieter Jelle Visser, Frederik Barkhof, and Bart N.M. van Berckel. Assessing amyloid pathology in cognitively normal subjects using ^{18}F-flutemetamol PET: Comparing visual reads and quantitative methods. *Journal of Nuclear Medicine*, 60(4):541–547, 2019.

[28] Lara García-Varela, David Vállez García, Manuel Rodríguez-Pérez, Aren Van Waarde, Jürgen W.A. Sijbesma, Anna Schildt, Chantal Kwizera, Pablo Aguiar, Tomás Sobrino, Rudi A.J.O. Dierckx, Philip H. Elsinga, and Gert Luurtsema. Test-Retest Repeatability of [^{18}F]MC225-PET in Rodents: A Tracer for Imaging of P-gp Function. *ACS Chemical Neuroscience*, 11(4):648–658, 2020.

[29] M. Muzi, D. A. Mankoff, J. M. Link, S. Shoner, A. C. Collier, L. Sasongko, and J. D. Unadkat. Imaging of Cyclosporine Inhibition of P-Glycoprotein Activity Using ^{11}C-Verapamil in the Brain: Studies of Healthy Humans. *Journal of Nuclear Medicine*, 50(8):1267–1275, aug 2009.

[30] Saskia P. Wolfensberger, Kaoru Maruyama, Bart N. van Berckel, Mark Lubberink, Anu J. Airaksinen, Ronald Boellaard, Gert Luurtsema, Wieb Reddingius, Frans E. Janssens, Dick J. Veltman, Albert D. Windhorst, Josée E. Leysen, and Adriaan A.

Lammertsma. Quantification of the neurokinin 1 receptor ligand [^{11}C]R116301. *Nuclear Medicine Communications*, 32(10):896–902, oct 2011.

[31] Adriaan A. Lammertsma. Forward to the Past: The Case for Quantitative PET Imaging. *Journal of Nuclear Medicine*, 58(7):1019–1024, jul 2017.

[32] B. N. M. van Berckel, Rik Ossenkoppele, Nelleke Tolboom, Maqsood Yaqub, Jessica C. Foster-Dingley, Albert D. Windhorst, Philip Scheltens, Adriaan A. Lammertsma, and Ronald Boellaard. Longitudinal Amyloid Imaging Using ^{11}C-PiB: Methodologic Considerations. *Journal of Nuclear Medicine*, 54(9):1570–1576, sep 2013.

[33] Débora E. Peretti, David Vállez García, Fransje E. Reesink, Tim van der Goot, Peter P. De Deyn, Bauke M. de Jong, Rudi A. J. O. Dierckx, and Ronald Boellaard. Relative cerebral flow from dynamic PIB scans as an alternative for FDG scans in Alzheimer's disease PET studies. *PLOS ONE*, 14(1):e0211000, jan 2019.

[34] Richard E Carson. Tracer Kinetic Modeling in PET. In *Positron Emission Tomography*, pages 127–159. Springer-Verlag, London, 2003.

[35] Roger N. Gunn, Steve R. Gunn, and Vincent J. Cunningham. Positron Emission Tomography Compartmental Models. *Journal of Cerebral Blood Flow & Metabolism*, 21(6):635–652, jun 2001.

[36] Adriaan A. Lammertsma and Susan P. Hume. Simplified Reference Tissue Model for PET Receptor Studies. *NeuroImage*, 4(3):153–158, 1996.

[37] Yanjun Wu and Richard E. Carson. Noise Reduction in the Simplified Reference Tissue Model for Neuroreceptor Functional Imaging. *Journal of Cerebral Blood Flow & Metabolism*, 22(12):1440–1452, 2002.

[38] Maqsood Yaqub, Nelleke Tolboom, Ronald Boellaard, Bart N M van Berckel, Erica W. van Tilburg, Gert Luurtsema, Philip Scheltens, and Adriaan A. Lammertsma. Simplified parametric methods for [11C]PIB studies. *NeuroImage*, 42(1):76–86, aug 2008.

[39] Roger N. Gunn, Adriaan A. Lammertsma, Susan P. Hume, and Vincent J. Cunningham. Parametric Imaging of Ligand-Receptor Binding in PET Using a Simplified Reference Region Model. *NeuroImage*, 6(4):279–287, 1997.

[40] O G Rousset, Y Ma, and A C Evans. Correction for partial volume effects in PET: principle and validation. *J Nucl Med*, 39(5):904–911, 1998.

[41] Andrea Pilotto, Enrico Premi, Silvia Paola Caminiti, Luca Presotto, Rosanna Turrone, Antonella Alberici, Barbara Paghera, Barbara Borroni, Alessandro Padovani, and Daniela Perani. Single-subject SPM FDG-PET patterns predict risk of dementia progression in Parkinson disease. *Neurology*, 90(12):e1029–e1037, mar 2018.

[42] K. Herholz, E. Salmon, D. Perani, J. C. Baron, V. Holthoff, L. Frölich, P. Schönknecht, K. Ito, R. Mielke, E. Kalbe, G. Zündorf, X. Delbeuck, O. Pelati, D. Anchisi, F. Fazio, N. Kerrouche, B. Desgranges, F. Eustache, B. Beuthien-Baumann, C. Menzel, J. Schröder, T. Kato, Y. Arahata, M. Henze, and W. D. Heiss.

Discrimination between Alzheimer dementia and controls by automated analysis of multicenter FDG PET. *NeuroImage*, 17(1):302–316, 2002.

[43] Phoebe G. Spetsieris, Yilong Ma, Vijay Dhawan, and David Eidelberg. Differential diagnosis of parkinsonian syndromes using PCA-based functional imaging features. *NeuroImage*, 45(4):1241–1252, 2009.

[44] David Eidelberg. Metabolic brain networks in neurodegenerative disorders: a functional imaging approach. *Trends in Neurosciences*, 32(10):548–557, oct 2009.

[45] Laura Teune, Fijanne Strijkert, Remco Renken, Gerbrand Izaks, Jeroen Vries, Marcel Segbers, Jos Roerdink, Rudi Dierckx, and Klaus Leenders. The Alzheimer's Disease-Related Glucose Metabolic Brain Pattern. *Current Alzheimer Research*, 11(8):725–732, sep 2014.